JACS
JOURNAL OF THE AMERICAN CHEMICAL SOCIETY

Communication

pubs.acs.org/JACS

Biphasic Self-Assembly Pathways and Size-Dependent Photophysical Properties of Perylene Bisimide Dye Aggregates

Franziska Fennel,[†] Steffen Wolter,[†] Zengqi Xie,[‡,§] Per-Arno Plötz,[†] Oliver Kühn,[†] Frank Würthner,*[,‡] and Stefan Lochbrunner*[,†]

[†]Institut für Physik, Universität Rostock, D-18051 Rostock, Germany

[‡]Institut für Organische Chemie and Center for Nanosystems Chemistry, Universität Würzburg, D-97074 Würzburg, Germany

Supporting Information

ABSTRACT: The concentration-dependent absorption and temperature-dependent fluorescence of the perylene bisimide dye PBI 1 in methylcyclohexane point to a biphasic aggregation behavior. At intermediate concentrations and temperatures, respectively, a dimer with low fluorescence yield dominates, which cannot be extended to longer aggregates. Those are formed at high concentrations and low temperatures, respectively, via a second, energetically unfavorable dimer species that acts as a nucleus. A corresponding aggregation model reproduces accurately the concentration dependence and allows extracting the equilibrium constants and spectra of the distinct species. The differences in the photophysical properties indicate H-type excitonic coupling for the favored dimer and J-type characteristics for the extended aggregates which could be related to structural models based on DFT calculations. The energetics can be understood by considering hydrogen-bonding and $\pi-\pi$-stacking interactions.

Since the seminal discovery by Jelley and Scheibe, dye aggregates have been established as valuable components for photonic applications.[1−4] In particular, the exciton transport properties[5] of some J-aggregates with red-shifted and narrowed absorption bands enable plasmonic hybrid systems and coupling to microcavity resonators,[6,7] and ultrahigh sensitivity to fluorescence-quenching analytes.[8] However, among the vast number of dye aggregates known, only a few proved their usefulness for such applications because the photophysical properties depend sensitively on the mutual arrangement of the chromophores in the respective aggregates. In general, aggregation can lead to red-shifted and narrowed absorption spectra and an increased radiative rate as well as to blue-shifted and broadened absorption spectra with reduced fluorescence quantum yields.[9,10] The former case is usually referred to as J- and the latter as H-aggregation.[9] Many dyes show both behaviors depending on the solvent,[11] the salt concentration,[12] or the pH value.[13] For any application, control of the aggregate structure and thereby of the associated photophysical properties is crucial and a quantitative description of the aggregation process most helpful. To this end, isodesmic or cooperative models[14] can be applied.[15,16] However, for many dyes these simple models cannot reproduce their aggregation behavior, calling for more sophisticated approaches.[17,18]

Here we investigate the concentration- and temperature-dependent aggregation behavior of the perylene bisimide[19] dye *N*,*N*-di[*N*-(2-aminoethyl)-3,4,5-tris(dodecyloxy)benzamide]-1,6,7,12-tetra(4-*tert*-butylphenoxy)perylene-3,4:9,10-tetracarboxylic acid bisimide (PBI 1, Scheme 1) and the associated photophysical properties in methylcyclohexane (MCH). Our interest was triggered by the observation of an unusual change of the fluorescence intensity upon increasing the concentration or varying the temperature, which pointed at a pronounced minimum for the fluorescence intensity for small aggregates. Accordingly, after an initial "aggregation-induced quenching", a subsequent "aggregation-induced emission"[20] behavior was observed upon further growth of the aggregate. In light of the strong recent interest in such phenomena,[21,22] we decided to carry out an in-depth study on the aggregation process, the involved aggregate species, and their photophysical characteristics.

Scheme 1. Chemical Structure of PBI 1

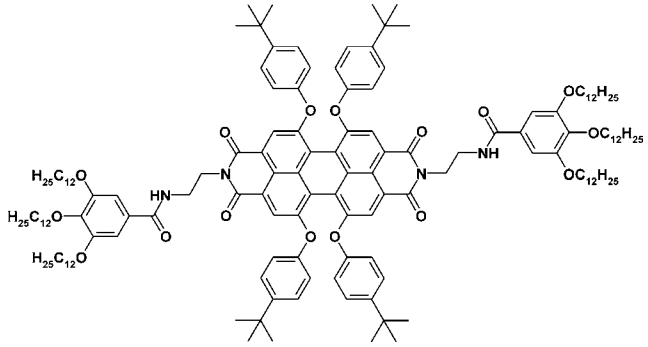

PBI 1 was synthesized as described in ref 23. Experimental details are given in the Supporting Information (SI). For our aggregation studies the nonpolar solvent MCH was used, which interacts only weakly with the dye. This ensures strong $\pi-\pi$-stacking interactions among the dyes with concomitant aggregate formation already at low concentrations and allows the application of gas-phase calculations to predict the supramolecular structures.

The apparent extinction coefficient per molecule of PBI 1 in MCH is shown in Figure 1a for a wide concentration range

Received: September 16, 2013
Published: December 9, 2013

   dx.doi.org/10.1021/ja409597x | *J. Am. Chem. Soc.* 2013, 135, 18722−18725

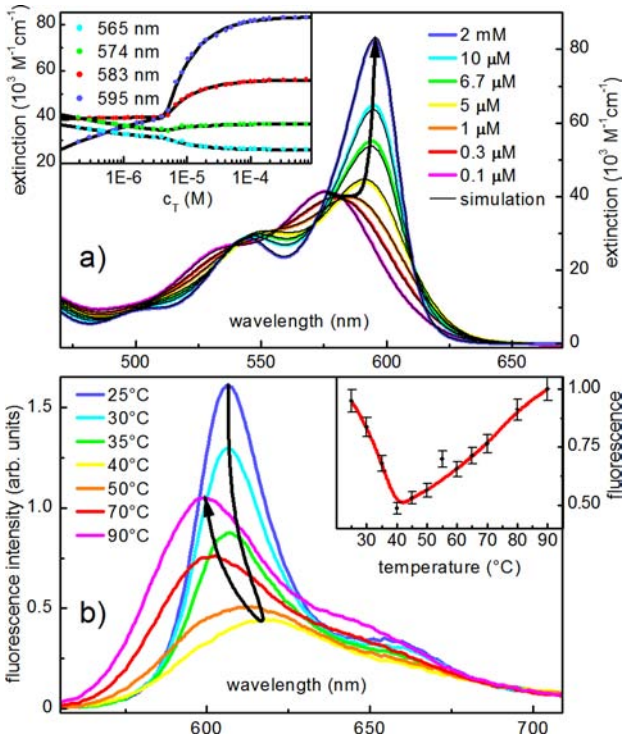

Figure 1. (a) Concentration-dependent measured (colored lines) and simulated (black lines) absorption spectra of PBI 1 in MCH at room temperature per molecule. The inset shows the measured (dots) and simulated (lines) concentration dependence of the absorption at specific wavelengths. (b) Temperature-dependent fluorescence spectra and normalized integrated yield (inset) of PBI 1 in MCH at a concentration of 0.02 mM. The red line serves as guide to the eye.

spanning 4 orders of magnitude. Starting from low concentrations, where the absorption is attributed to monomers, the main absorption band in the visible spectral region shifts with increasing concentration by 19 nm toward the red. Further increasing the concentration results in the growth of the lowest energy band and narrowing of the spectral features. The lack of isosbestic points but the presence of several isosbestic regions indicate that at least three species with distinct spectral properties—the monomer, an intermediate, and the fully developed aggregates—contribute to the overall absorbance. This can be also seen from the absorption at specific wavelengths (Figure 1a, inset), which exhibits two distinct regimes of wavelength-dependent spectral evolution with concentration.

Likewise, the fluorescence spectra of PBI 1 in MCH at a concentration of 0.02 mM show a biphasic temperature dependence (Figure 1b). Heating from room temperature, where extended aggregates with small Stokes shift (11 nm) prevail, leads to a dissociation into monomers with large Stokes shift (29 nm) at the highest temperature of 90 °C, similar to what was observed for other PBI dye aggregates.[24] The final state at 90 °C also shows all spectral characteristics of related monomeric perylene bisimide dyes bearing four phenoxy substituents in the bay region.[25,26] More interestingly, however, are the observations for temperatures between the extremes. Thus, in the interval from 25 to 40 °C, the sharp emission band loses its intensity and shifts slightly to the red, concomitant with a decrease of the quantum yield by almost a factor of 2 (Figure 1b, inset). In the next interval from 40 to 90 °C, however, a turnaround is observed with an increase of the fluorescence quantum yield even slightly above the initial value. This process is further characterized by a spectral shift to the blue and the reappearance of vibronic structure.

A similar behavior but with different transition temperatures is observed at other concentrations of PBI 1 (see SI). Lowering the concentration shifts the configuration with the minimal quantum yield and strongest red shift to lower temperatures, while higher concentrations are associated with a temperature increase for the formation of these spectral features. Accordingly, we conclude that the quantum yield and the spectral shift of the fluorescence depend primarily on the size of the aggregates and only indirectly on the temperature. To explain the findings, a third species besides the monomers and the final aggregates has to be considered, which dominates at intermediate temperatures and exhibits a lower quantum yield and a red-shifted fluorescence spectrum. The fluorescence properties point to aggregates with H- or even excimer-type characteristics, since in this case the transition to the lowest electronically excited state carries no or only small oscillator strength, and they exhibit typically broad absorption and fluorescence bands as well as a comparably large Stokes shift. The findings seem to indicate that aggregation of PBI 1 leads first to small aggregates, respectively dimers, with little oscillator strength in the lowest excitonic states. Only upon further growth into larger aggregates is an aggregate species with increased transition dipoles for the lowest excited state formed.

The observed behavior is clearly more complex than expected for a simple isodesmic or even the more sophisticated nucleation–elongation growth model.[15,16] In the former case the aggregate would develop from the monomer by addition of one molecule after the other, and the spectra could be decomposed into monomer and aggregate contributions, which was clearly not possible here. We also tried to analyze the concentration dependence with an anti-cooperative aggregation model[15,16] in which the dimerization constant is larger than the growth constant of the successive aggregation steps. However, also here no satisfactory agreement with the measurements was achieved. Guided by the notion that the dimer has quite different photophysical properties compared to the longer aggregates, the model depicted in Figure 2 is therefore proposed, which complies with all our observations.

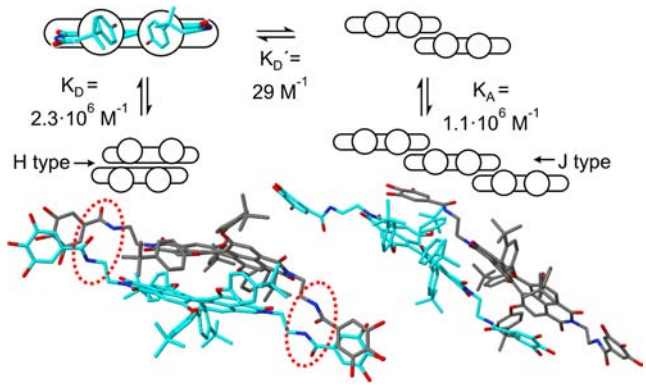

Figure 2. Proposed aggregation model and calculated structures of the favored dimer and the dimer acting as nucleus for the aggregates. The dodecyl chains are omitted in the figure but taken into account in the calculations. The red circles mark the area where hydrogen bonds are suggested.

dx.doi.org/10.1021/ja409597x | J. Am. Chem. Soc. 2013, 135, 18722–18725

The model is based on the appearance of two dimeric species. One, D, is responsible for the spectra at intermediate concentrations and temperatures, respectively. It is energetically favored and forms from monomers M with a high dimerization constant, K_D:

$$M + M \rightleftharpoons D; \quad [D] = K_D[M]^2 \tag{1}$$

However, this species D cannot provide the required contact surface for the association of a third monomer for reasons discussed below. On the other hand, a second energetically unfavored dimer D′ which is formed only in minor amounts due to its lower dimerization constant K_D' can be extended by a third and a fourth molecule at its periphery and accordingly acts as a nucleus for longer aggregates. The concentration of D′ is again given by eq 1, but with the constant K_D'. The growth of larger aggregates M_n is described by the successive association of monomers with the aggregation constant K_A:

$$M_{n-1} + M \rightleftharpoons M_n;$$
$$[M_n] = K_A[M_{n-1}][M] = K_A{}^{n-2}K_D'[M]^n \tag{2}$$

Here M_2 is identified with the second dimer D′. Introducing the total concentration $c_T = c_M + c_D + c_A$ of dye molecules, with the concentration $c_M = [M]$ of monomers, $c_D = 2[D]$ of dye molecules in the favored dimers, and c_A of molecules in unfavored dimers and in particular in larger aggregates, one finds the following relations between the monomer concentration and those of the other species:

$$c_D = 2K_D c_M{}^2 \tag{3}$$

$$c_A = \frac{K_D'}{K_A}\left(\frac{1}{(1 - K_A c_M)^2} - 1\right)c_M \tag{4}$$

$$c_T = c_M + 2K_D c_M{}^2 + \frac{K_D'}{K_A}\left(\frac{1}{(1 - K_A c_M)^2} - 1\right)c_M \tag{5}$$

Using a fit algorithm, which minimizes the quadratic error, the aggregation constants and absorption spectra of dye molecules in the monomeric form, in dimers, and in larger aggregates are extracted. Details are given in the SI. The obtained aggregation constants for the self-assembly of PBI 1 in MCH at room temperature are $K_D = 2.3 \times 10^6\ M^{-1}$, $K_D' = 29\ M^{-1}$, and $K_A = 1.1 \times 10^6\ M^{-1}$. Figure 3 shows the spectra of the distinct species and the simulated fractions $\alpha = c/c_T$ as a function of the total concentration. The favored dimer aggregate accumulates at intermediate concentrations. This behavior is comparable to the prevalence of cyclic species in one-dimensional self-assemblies below the so-called effective molarity concentration.[27] Due to the small aggregation constant K_D', the proportion of the unfavored dimer is always negligible, and long J-aggregates are formed immediately at higher concentrations. Therefore, the unfavored dimer never contributes significantly to the spectra. The long aggregates (blue in Figure 3) show all typical signatures of J-aggregates, while the favored dimer (red) may be classified as an H-aggregate despite some peculiarities. Thus, the lack of a blue shift indicates that the exciton coupling is weak and the "gas-to-crystal red shift"[9] overcompensates the aggregation-induced blue shift. Excellent agreement between measurements and simulated absorption spectra is achieved, as can be seen from the comparison of experimental (color) and simulated (black) data in Figure 1a.

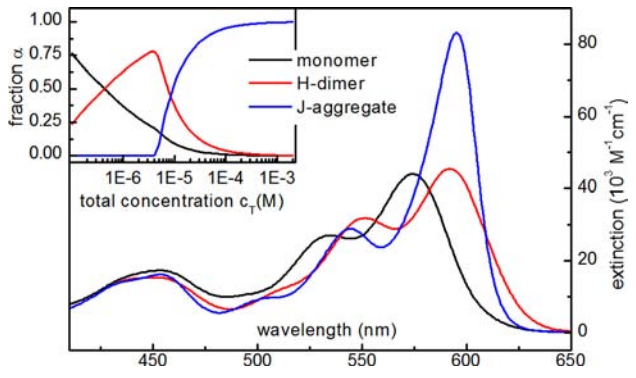

Figure 3. Spectra of the monomer, favored H-dimer, and larger J-aggregates extracted from the aggregation model. The inset shows the fraction of monomers, molecules in the favored H-dimer, and molecules in J-aggregates as a function of the total dye concentration.

The appearance of two dimers is supported by quantum chemical calculations (simulated annealing molecular dynamics using density functional based tight-binding[28] including empirical dispersion corrections[29] as implemented in the DFTB+ package[30]) of stacked and laterally shifted dimer structures as shown in Figure 2. To relate the thermodynamic and spectroscopic information obtained for PBI 1 monomer, dimers, and extended aggregates to supramolecular structures, we have to consider the twisted nature of the PBI backbone with conformationally flexible phenoxy substituents as well as the hydrogen bond donating (NH) and accepting (O) site at each of the two benzamide groups tethered to the imide substituents. The fact that the K_D value of PBI 1 is more than 3 orders of magnitude larger than those observed for related PBI dyes without peripheral benzamide subunits[24] supports the involvement of hydrogen bonds in the energetically favored dimer. The second dimer is disfavored as expressed by a 4 orders of magnitude smaller aggregation constant K_D'. This is caused by the weaker binding energy resulting from a lateral shift of the two monomers with respect to each other giving rise to a reduced influence of the hydrogen bonds and only partial $\pi-\pi$ contact. However, the lateral shift leads to a sterically less restricted structure which allows an extension by further monomers. Such a lateral shift is similar to that observed for another PBI J-aggregate reported previously.[31] We note that the elongation constants K_A of the two systems are almost identical, corroborating the idea of a similar slipped-stack arrangement. The major difference is that the structural features of our earlier system did not support the formation of an alternative favored dimer species, and accordingly the simple nucleation−growth model was applicable.

Similar situations might be encountered more frequently than one would assume on first sight. The structure of dimers is determined by the best mutual interaction between the two involved molecules, which calls for "induced-fit" optimization of two adjacent van der Waals surfaces. This optimization can go along with a strong penalty for the association of a third molecule, e.g., by orientation of all eight phenoxy groups away from the $\pi-\pi$ contact surfaces in the case of PBI 1. As a consequence, the dimer unit has to be rearranged or another dimer with a different geometry has to be formed before association of a third and fourth molecule can take place on the other side of the π-scaffolds. This structure is less favorable than the optimized dimer but can act as seed for the growth of larger aggregates. Whenever the difference in free energy between

dx.doi.org/10.1021/ja409597x | J. Am. Chem. Soc. 2013, 135, 18722−18725

these two dimers becomes significant, the situation is related to the one described here, and the proposed aggregation scheme as well as our mathematical treatment should be applicable. For instance, for PIC molecules, Scheibe described 75 years ago the formation of dimers with distinct optical properties before J-aggregates are formed at higher concentration.[32]

In summary, we observed two aggregation pathways for PBI 1, leading to different sizes and mutual arrangements of the building blocks. At intermediate concentrations and temperatures, a compact sandwich-type dimer species with H-type excitonic character, in particular with aggregation-induced quenching behavior, dominates which cannot grow into extended aggregates. Growth into larger aggregates with J-type excitonic character and enhanced fluorescence is, however, possible from a less favored dimer nucleus and experimentally observed at high concentrations (and/or lower temperatures). Based on a newly derived aggregation model, the observed concentration and temperature dependences could be described quantitatively. Therefore, this study contributes to the understanding of pathway-dependent self-assembly processes[33,34] and aggregate structure−fluorescence relationships,[20] which are both very active fields of current research.

■ ASSOCIATED CONTENT

Ⓢ Supporting Information

Experimental details and supporting results. This material is available free of charge via the Internet http://pubs.acs.org.

■ AUTHOR INFORMATION

Corresponding Authors

wuerthner@chemie.uni-wuerzburg.de
stefan.lochbrunner@uni-rostock.de

Present Address

[§]Z.X.: South China University of Technology, Guangzhou 510640, China

Notes

The authors declare no competing financial interest.

■ ACKNOWLEDGMENTS

Financial support by the German Science Foundation via the collaborative research center SFB 652 "Strong correlations and collective effects in radiation fields: Coulomb systems, clusters and particles" and the research group FOR 1809 "Light-induced dynamics in molecular aggregates" is gratefully acknowledged.

■ REFERENCES

(1) Wasielewski, M. R. *Acc. Chem. Res.* **2009**, *42*, 1910−1921.
(2) Würthner, F.; Kaiser, T. E.; Saha-Möller, C. R. *Angew. Chem., Int. Ed.* **2011**, *50*, 3376−3410.
(3) Kobayashi, T., Ed. *J-aggregates*; World Scientific: Hackensack, NJ, 2012; Vol. *2*.
(4) Eisele, D. M.; Knoester, J.; Kirstein, S.; Rabe, J. P.; Vanden Bout, D. A. *Nature Nanotech.* **2009**, *4*, 658−663.
(5) Scheblykin, I. G.; Sliusarenko, O. Y.; Lepnev, L. S.; Vitukhnovsky, A. G.; Van der Auweraer, M. *J. Phys. Chem. B* **2001**, *105*, 4636−4646.
(6) Salomon, A.; Genet, C.; Ebbesen, T. W. *Angew. Chem., Int. Ed.* **2009**, *48*, 8748−8751.
(7) Tischler, J. R.; Bradley, M. S.; Bulovic, V.; Song, J. H.; Nurmikko, A. *Phys. Rev. Lett.* **2005**, *95*, 036401.
(8) Achyuthan, K. E.; Bergstedt, T. S.; Chen, L.; Jones, R. M.; Kumaraswamy, S.; Kushon, S. A.; Ley, K. D.; Lu, L.; McBranch, D.; Mukundan, H.; Rininsland, F.; Shi, X.; Xia, W.; Whitten, D. G. *J. Mater. Chem.* **2005**, *15*, 2648−2656.
(9) Spano, F. C. *Acc. Chem. Res.* **2010**, *43*, 429−439.
(10) Kasha, M.; Rawls, H. R.; Ashraf El-Bayoumi, M. *Pure Appl. Chem.* **1965**, *11*, 371−392.
(11) Shirakawa, M.; Kawano, S.; Fujita, N.; Sada, K.; Shinkai, S. *J. Org. Chem.* **2003**, *68*, 5037−5044.
(12) Slavnova, T.; Chibisov, A.; Görner, H. *J. Phys. Chem. A* **2005**, *109*, 4758−4765.
(13) Egawa, Y.; Hayashida, R.; Anzai, J.-I. *Langmuir* **2007**, *23*, 13146−13150.
(14) Isodesmic: all binding events are characterized by the same binding constant. Cooperative: first a nucleus is formed by self-assembly with a smaller aggregation constant.
(15) De Greef, T. F. A.; Smulders, M. M. J.; Wolffs, M.; Schenning, A. P. H. J.; Sijbesma, R. P.; Meijer, E. W. *Chem. Rev.* **2009**, *109*, 5687−5754.
(16) Chen, Z.; Lohr, A.; Saha-Möller, C. R.; Würthner, F. *Chem. Soc. Rev.* **2009**, *38*, 564−584.
(17) Bellot, M.; Bouteiller, L. *Langmuir* **2008**, *24*, 14176−14182.
(18) Miraldi, E. R.; Thomas, P. J.; Romberg, L. *Biophys. J.* **2008**, *95*, 2470−2486.
(19) Weil, T.; Vosch, T.; Hofkens, J.; Peneva, K.; Müllen, K. *Angew. Chem., Int. Ed.* **2010**, *49*, 9068−9093.
(20) Hong, Y.; Lam, J. W. Y.; Tang, B. Z. *Chem. Commun.* **2009**, 4332−4353.
(21) Chan, J. M. W.; Tischler, J. R.; Kooi, S. E.; Bulovic, V.; Swager, T. M. *J. Am. Chem. Soc.* **2009**, *131*, 5659−5666.
(22) Karunakaran, V.; Prabhu, D. D.; Das, S. *J. Phys. Chem. C* **2013**, *117*, 9404−9415.
(23) Li, X.-Q.; Zhang, X.; Ghosh, S.; Würthner, F. *Chem.—Eur. J.* **2008**, *14*, 8074−8078.
(24) Chen, Z.; Baumeister, U.; Tschierske, C.; Würthner, F. *Chem.—Eur. J.* **2007**, *13*, 450−465.
(25) (a) Fennel, F.; Lochbrunner, S. *Phys. Chem. Chem. Phys.* **2011**, *13*, 3527−3533. (b) Ambrosek, D.; Marciniak, H.; Lochbrunner, S.; Tatchen, J.; Li, X.-Q.; Würthner, F.; Kühn, O. *Phys. Chem. Chem. Phys.* **2011**, *13*, 17649.
(26) Hofkens, J.; Vosch, T.; Maus, M.; Köhn, F.; Cotlet, M.; Weil, T.; Herrmann, A.; Müllen, K.; De Schryver, F. *Chem. Phys. Lett.* **2001**, *333*, 255−263.
(27) Hunter, C. A.; Anderson, H. L. *Angew. Chem., Int. Ed.* **2009**, *48*, 7488−7499.
(28) Elstner, M.; Porezag, D.; Jungnickel, G.; Elsner, J.; Haugk, M.; Frauenheim, T.; Suhai, S.; Seifert, G. *Phys. Rev. B* **1998**, *58*, 7260−7268.
(29) Elstner, M.; Hobza, P.; Frauenheim, T.; Suhai, S.; Kaxiras, E. *J. Chem. Phys.* **2001**, *114*, 5149−5155.
(30) Aradi, B.; Hourahine, B.; Frauenheim, T. *J. Phys. Chem. A* **2007**, *111*, 5678−5684.
(31) Kaiser, T. E.; Stepanenko, V.; Würthner, F. *J. Am. Chem. Soc.* **2009**, *131*, 6719−6732.
(32) Scheibe, G. *Kolloid-Z.* **1938**, *82*, 1−14.
(33) Tidhar, Y.; Weissman, H.; Wolf, S. G.; Gulino, A.; Rybtchinski, B. *Chem.—Eur. J.* **2011**, *17*, 6068−6075.
(34) Jonkheijm, P.; van der Schoot, P.; Schenning, A. P. H. J.; Meijer, E. W. *Science* **2006**, *313*, 80−83.